# Damage Identification of Continuous Rigid Frame Concrete Bridge

Shengnan Huang[1,*], Lieping Ye[2] and Xinzheng Lu[2]

[1]*Civil and Environmental Engineering Institute, University of Science and Technology Beijing, Beijing 100083, China*

[2]*Key Laboratory of Civil Engineering Safety and Durability of Ministry of Education, Department of Civil Engineering, Tsinghua University, Beijing 100084, China*

**Abstract:** During a bridge service life, many factors can cause damage accumulation such as overloaded traffic, fatigue effect, and so on. Hence, the identification of potential damages has been received wide attention to prevent such sudden fatal accident. An experiment of a continuous rigid frame concrete bridge, which had 3 spans and a total length of 18 meters, was presented in this paper. Two load stages and ten different load steps were simulated to test various scenario of long-term loading and different levels of overload. Curvature mode method was adopted to detect the damage during the exercises. The changes of curvature modes were used to detect damage after the ten load steps. This method performed excellent to identify the damage position of the bridge. So, it is concluded that the curvature modes can be used to detect damage in actual structures. In addition, the Finite-Element Analysis (FEA) was utilized, and the experimental recurring was verified positively through FEA model.

**Keywords:** Bridge, curvature mode, damage identification, dynamic fingerprint, experimental study, FEA.

## INTRODUCTION

During a bridge service life, many factors can cause damage accumulation such as overloaded traffic, fatigue effect, and so on. In the last few decades in China, over loading becomes a common phenomenon, which brings serious safety problem to the bridges. Each year, it is reported that the sudden failures of bridges have induced serious financial lost, sometime even human death. The safety monitoring system is a solution method to prevent sudden failure of bridges [1]. In a health monitoring system, there are three key issues, damage identification, damage location, and damage quantification.

Many damage detection methods have been proposed by different researchers [2-4]. The dynamic fingerprint method was widely used in real structures, such as frequency, flexibility matrix, curvature mode, and so on.

Frequency which was the global parameter could be used to detect damage. In 1975, resonant frequency was used to detect damage by Vandiver [5]. Adams *et al.* demonstrated that the decrease of natural frequency and the increase of damping could be used as damage index in fiber-reinforced plastics [6]. The same method was adopted on a highway bridge and in offshore structures by Biswas *et al*. [7], Loland and Dodds [8], and Vandiver [5].

Frequency response functions (FRFs) was another method to detect damage suggested by Samman and Coworkers [9-12]. Damage could be identified through comparing the FRFs between the intact and damaged structures. Such method had successfully detected damage in a laboratory model bridge by Samman and Coworkers. In 2000, Cha and Tuck-Lee [13] used FRFs to update the structural parameters.

Stiffness was the most direct damage index, so Mannan and Richardson utilized the difference of the stiffness matrix between the intact and damaged structures to detect damage [14]. Then stiffness error matrix method was proposed for large stiffness change, and weighted-error-matrix method was used for small stiffness change suggested by Park *et al*. [15]. However high mode played an important role in stiffness matrix found by Lin [16], so the precondition was that all modes could be obtained, at least enough modes could be tested [17].

To solve this problem, flexibility matrix which was the inverse of stiffness matrix was adopted as damage index. Pandey and Biswas found that it was viable to use changes in the flexibility matrix of structure to locate damage in beams [18]. Only a few of the lower frequency modes were needed to estimate flexibility matrix studied by Pandey and Biswas [18, 19]. Rubin and Coppolino proposed a method which was used a normalized flexibility parameter to monitor offshore platforms [20]. In besides, a damage location vector (DLV), which was computed through the change of flexibility matrix, was put forward by Bernal [21, 22].

To locate damage more accurately, power spectral densities and curvature of mode shapes was proposed [23, 24]. These methods were applied on bridges by Sikorsky and Stubbs [25]. It was concluded that the curvature of mode

*Address correspondence to this author at the Civil and Environmental Engineering Institute, University of Science and Technology Beijing, Beijing 100083, China; Tel:(+86)13810593480;
E-mail: huangcn03@mails.tsinghua.edu.cn

1874-1495/14 2014 Bentham Open

shapes was sensitive to damage in beam structures. With this understanding, Curvature Damage Factor (CDF), which was the average of curvature changes in all modes, was used by Wahab [26].

In this paper, an experiment of a continuous rigid frame (CRF) concrete bridge, which had 3 spans and a total length of 18 meters, was presented. Two load stages and ten different load steps were simulated to test various scenario of long-term loading and different levels of overload. The curvature mode was used to detect damage, especially based on either intact structures or damaged structures.

Curvature mode could be obtained by two methods, either from the displace mode or from the strain responses [27-29]. In this paper, the curvature mode was calculated through (1), and the damage index which was used to identify damage position was calculated through (2).

$$\phi_j = \frac{u_{j-1} - 2u_j + u_{j+1}}{(l_j / l_0)^2} \tag{1}$$

$$I_u = \left|\Delta\phi_j\right| \tag{2}$$

In these formulae, $\varphi_j$ was the curvature mode of point $j$, $u_j$ was the displace mode of point $j$, $l_j$ was the distance between two test points, $l_0$ was the reference distance, $I_u$ was the damage index.

## EXPERIMENT MODEL AND TEST SCHEME

The CRF bridge model was shown in Fig. (**1**). It had three spans, and the total length was 18.25 m. The dimension was 1/4 of the actual bridge. To make sure that the test model and the actual bridge had the same stress distribution under gravity load, 3 kN/m of uniform load was put on the top of the model, shown as Fig. (**2**).

**Fig. (2).** The uniform load on the top of the model.

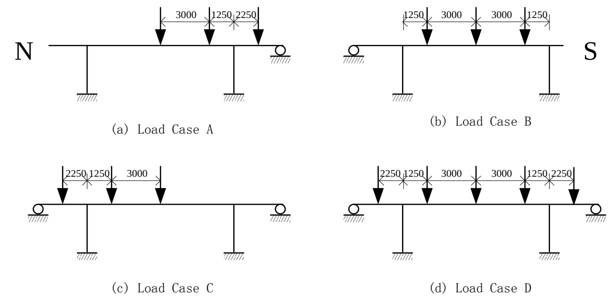


**Fig. (3).** Loading patterns.

There were two loading stages in the experiment. The first one was long-term loading, which was for the research of shrinkage and creep. The second one was running simulating load stage. In the second stage, five oil jacks were used. There were four load patterns shown in Fig. (**3**). From load case A to load case C, the vehicle running process was simulated. Load case D was the destroyed loading process. The loading detail was listed in Table **1**.

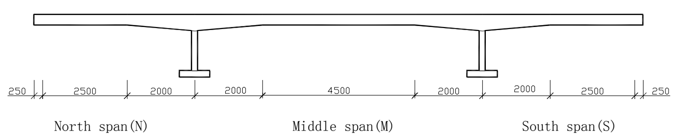


**Fig. (1).** The test model.

**Table 1. Load scheme.**

| Load Step | Load Case | Load or Deformation Level | Working Status |
|---|---|---|---|
| 1 | A | Each jack load is 37.5 kN. | Service state |
| 2 | B | | |
| 3 | C | | |
| 4 | A | Each jack load is 55 kN. | Overloading |
| 5 | B | Each jack load is 50 kN. | |
| 6 | C | Each jack load is 55 kN. | |
| 7 | D | Each jack load is 37.5 kN. | Service state |
| 8 | | Maximum deformation arrives 28.3 mm | Overloading |
| 9 | | Maximum deformation arrives 60 mm | Seriously damaged |
| 10 | | Maximum load | Destroyed |

After every load step, the dynamic test was carried, and the dynamic fingerprints were obtained to detect damage.

## EXPERIMENTAL PHENOMENA

In the first loading stage, the long-term loading was carried by putting 3 tons weight in the middle of the bridge (Fig. **4**). The long-term loading was persisted for 832.8 hrs, and the deformation in this stage was shown in Fig. (**5**). In this figure, the jumping-off point of the abscissa was the moment before prestressing. So the displacement after prestressing was minus which means the displacement was upwards. It was obviously that creep developed relaxedly during the long-term testing. Under this load stage, visible cracks were founded at the mid-span of the bridge. However, some of the cracks closed after the weight moved away.

In the second loading stage, there were ten load steps. The typical phenomena were listed in Table **2**.

Load step 1-3 monitored the service state (Fig. **6**). Most of the flexural cracks fully propagated during load step 1-3. In load step 1, when the load of each oil jack arrived at 30 kN the cracks in the south span appeared. At the end of load step 1, the crack in the south span developed equably, the crack width was 0.05 mm, the space between cracks was from 150 mm to 200 mm. In load step 2, when the load of each oil jack arrived at 22 kN, the supports in the two side span turned up, and it resulted in the stiffness decreasing. In load step 3, when the load of each oil jack arrived at 10 kN the crack appeared on the top of the north pier. In this step, the stiffness was almost the same as load step 1.

Load step 4-6 monitored the over loading state (Fig. **7**). In load step 4, followed by the increasing of the load the stiffness of the bridge decreased. At the end of this load step, the steel strain in the middle span arrived at 983με. Load step 5 was tested in term of load case B which was the worst load case. When the load of each oil jack arrived at 20 kN, the supports in the two side span turned up. At the load of 45 kN, the normal steel reinforcement progressively yielded, whilst the tendon was still elastic. Because of the damage caused by load step 5, the stiffness reduced compared with load step 4.

**Fig. (4).** The long-term loading.

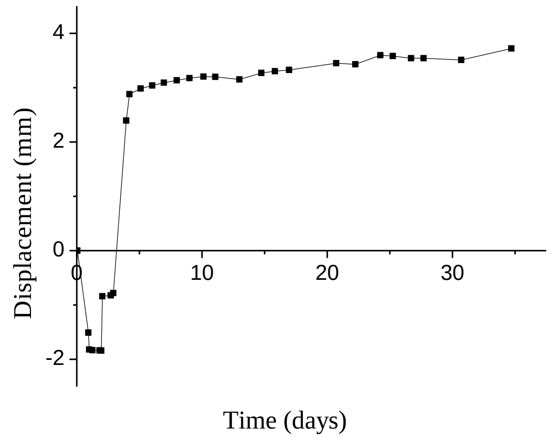


**Fig. (5).** The creep development.

**Table 2. Typical phenomena.**

| Loading State | Load Step | Maximal Crack Width / mm | Steel Strain in the Mid-span / με | Deflection in the Mid-span / mm | Residual Deflection in Mid-span / mm |
|---|---|---|---|---|---|
| Long-term loads | — | 0.02 | | | |
| Vehicle loads | 1 | 0.05 | 312 | 4.8 | 0.15 |
| | 2 | 0.10 | 872 | 12.5 | 0.65 |
| | 3 | 0.10 | 533 | 6.1 | 0.66 |
| | 4 | 0.15 | 983 | 11.4 | 0.82 |
| | 5 | 0.25 | 1726 | 35.5 | 2.13 |
| | 6 | 0.25 | 922 | 17.0 | 2.38 |
| | 7 | 0.30 | 493 | 10.1 | 2.43 |
| | 8 | | 1622 | 28.5 | 4.89 |
| | 9 | | yielded | 60.2 | 26.35 |
| | 10 | | | 154.2 | Destroyed |

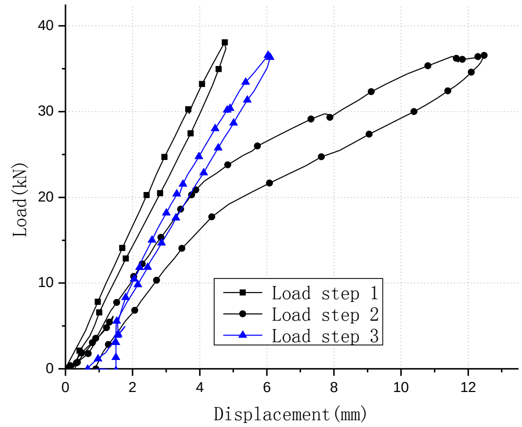


**Fig. (6).** Load-deflection at the mid-span from load step 1 to 3.

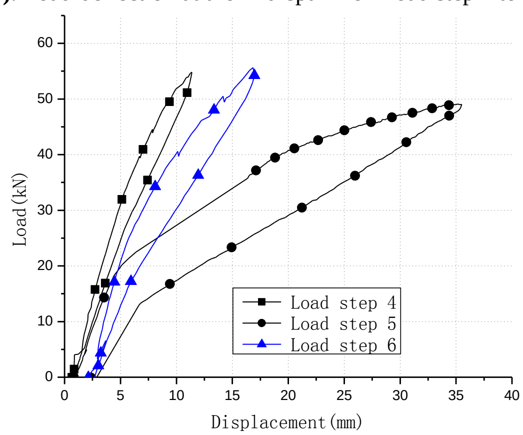


**Fig. (7).** Load-deflection at the mid-span from load step 4 to 6.

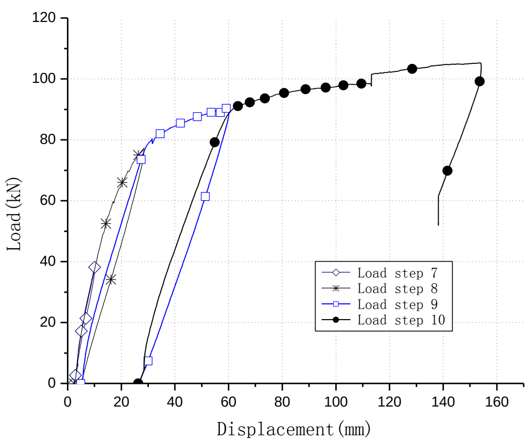


**Fig. (8).** Load-deflection at the mid-span from load step 7 to 10.

Load step 7-10 was destructive loading stage (Fig. **8**). In load step 7, at the load of 37.5 kN, the deflection in the middle of the middle span arrived at 10 mm, and the crack width was 0.3 mm. From load step 8 to load step 10, the concrete crack developed and the steel yielded in succession, so the stiffness of the bridge decreased gradually. At the load of 80 kN, the steel in the middle of the middle span yielded, so there was a turning point in the load-deflection relationship. Some cracks developed throughout the whole section. The bridge didn't collapse because of the prestressed tendons.

## SAFETY MONITORING AND DAMAGE DETECTION

### Damage Detection in Long-term Loading

During the construction process, the dynamic tests were carried after every procedure, and the test results were shown in Table **3**. The state after adding uniform load which was the same as the state of the real bridge was adopt as the intact state, and all of the damage analyses was based on this state.

After long-term loading, the frequency decreased because of the crack of concrete. To locate the position of the damage, the curvature mode change was calculated (Fig. **9**). The peak value of the damage index was in the middle of the middle span, which was in accordance with the crack position. So curvature mode was successfully to detect damage in this stage.

### Damage Detection in Service Loading and Overloading

Fig. (**10**) showed the frequency change in the second loading stage. From load step 1 to load step 8, the frequency decreased, which meant that the damage developed and the stiffness reduced. However, in the moderately overloading stage the amplitude of frequency variation was too small to detect damage. After load step 8, when the damage was serious, the frequency decreased obviously. So frequency was insensitive to detect damage for overloading.

Another dynamic fingerprint such as curvature mode, which was calculated through (1), was also used to detect damage. From load step 1 to load step 6, the damage index of curvature mode was shown in Figs. (**11**, **12**).

In Fig. (**11**), after load step 1, the peak value of the damage index in the mid-span was almost the same as it was after long-term loading (Fig. **9**). In the south span, the peak value of the damage index increased caused by the propagation of flexural cracks. After load step 2, the peak value of the damage index in the north span increased obviously. It was because that load step 2 was the most unfavorable load pattern, and the section on the top of the north pier cracked. After load step 3, the dynamic characteristics were not tested.

Fig. (**12**) showed the damage index change from load step 4 to load step 6. In this loading stage, the bridge was in

**Table 3. Frequency test results.**

| State | Before Prestressed | After Prestressed | Add Uniform Load | After Long-term Load |
|---|---|---|---|---|
| 1st mode / Hz | 15.62 | 15.62 | 11.12 | 10.87 |
| 2nd mode / Hz | 32.87 | 32.87 | 23.5 | 23.12 |

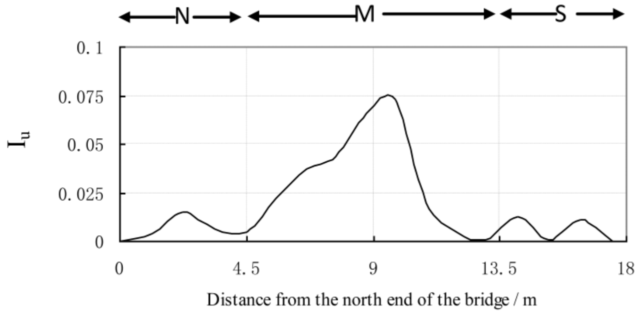


**Fig. (9).** Damage index change after long-term loading.

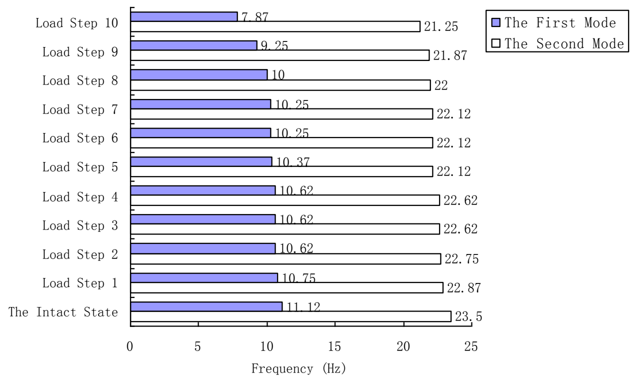


**Fig. (10).** Frequency test results.

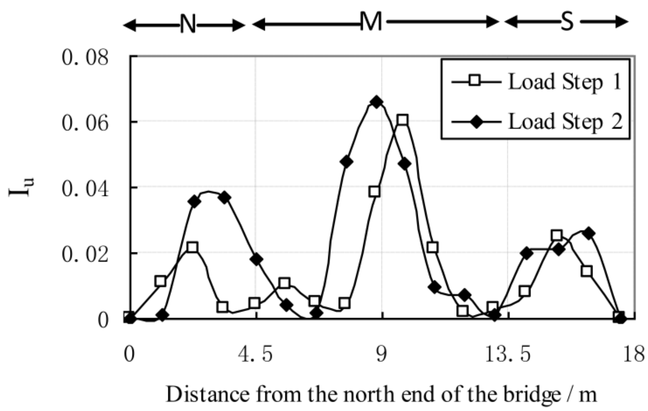


**Fig. (11).** Damage index change from load step 1 to load step 2.

the state of overload. After load step 4, the peak value of damage index in the north span increased to 0.05, which meant that the damage aggravated under overloading state. In load step 5, the peak value of the damage index was in the middle of the mid-span. During this loading process, the steel of the north pier yielded, which led to the stiffness decrease. So after load step 6, the damage index changed obviously in the whole bridge. In Fig. (**12**), it could be seen that the damage developed from the north span to the south span, which was consistent with the loading process.

## Damage Detection in Destructive Loading

In load step 7, each jack load arrived at 37.5 kN, and the damage was no further development. So after this load step, the dynamic characteristics were not tested.

From load step 8 to load step 9, the cracks was obviously, and the steels in the bridge had yielded. So in this loading stage, the stiffness of the bridge decreased seriously, and the deflection of the bridge was visible. After load step 10, the bridge was destroyed.

In destructive loading stage, the peak value of the damage index increased, but it was not obvious. It was because that the cracks had fully developed, and the steels had yielded after load step 6. In this stage, the stiffness change was small due to cracking and yielding. So the damage index of curvature mode was insensitive.

## Damage Detection Based on Damaged Bridge

For actual bridges, it was difficult to obtain the curvature mode of the original state. In service period, the bridge was working with cracks. So the damage identification results based on damaged structures were discussed in this section.

The curvature mode tested after long-term loading was used as the reference state in load step 1 and load step 2. The damage index results were shown in Fig. (**13**). It could be found that after load step 1 the peak value of damage index was in the south span and in the mid-span. After load step 2, the damage in the mid-span and in the north span further developed. The degree of the damage index differences was larger compared with Fig. (**11**).

The curvature mode tested after load step 2 was used as the reference state from load step 4 to load step 6, and the calculated results were shown in Fig. (**14**). It could be seen that the damage developed from the north span to the south span, which was consist with the loading process.

During the destructive loading stage, the working state after load step 8, which was almost the same as it was after

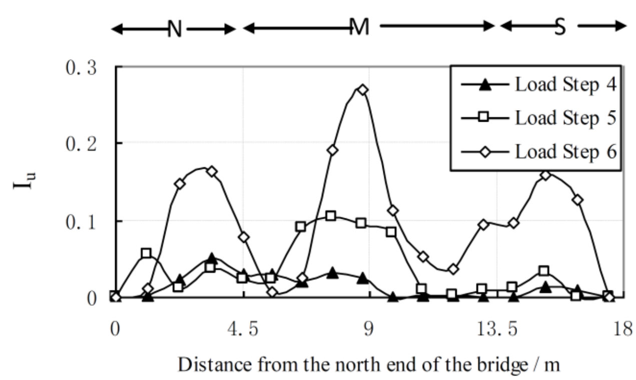


**Fig. (12).** Damage index change from load step 4 to load step 6.

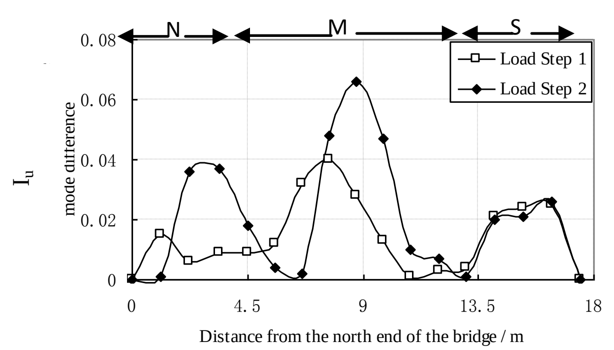


**Fig. (13).** Relative damage index change from load step 1 to load step 2.

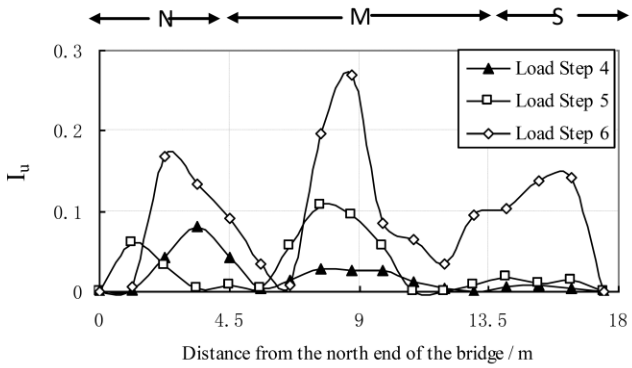


**Fig. (14).** Relative damage index change from load step 4 to load step 6.

load step 6, was used as the reference state. The calculated results were shown in Fig. (**15**). It could be seen that the damage position was in the middle of each span. The peak value of the damage index enhanced from load step 9 to load step 10, which meant the damage degree increased. However, the damage identification capability of curvature mode decreased when the damage was serious.

## FINITE-ELEMENT ANALYSIS

In order to analyze the mechanical behavior of the model bridge, a finite-element model was established using the software MSC.Marc. To monitor the bending deformation which was the main behavior of the model bridge, plane stress elements and two dimension rebar elements were used. Contact cells were adopted in the support, to monitor the supporting behavior which only bore press. Many nonlinear behaviors were considered in this finite-element model, such as cracking and yielding.

The calculated results were shown in Fig. (**16**). It was shown that the finite element calculation results agreed well with the experimental results. Further analysis could be expanded based on this finite-element model.

## CONCLUSION

In this paper, an experiment of a continuous rigid frame concrete bridge, which had 3 spans and a total length of 18

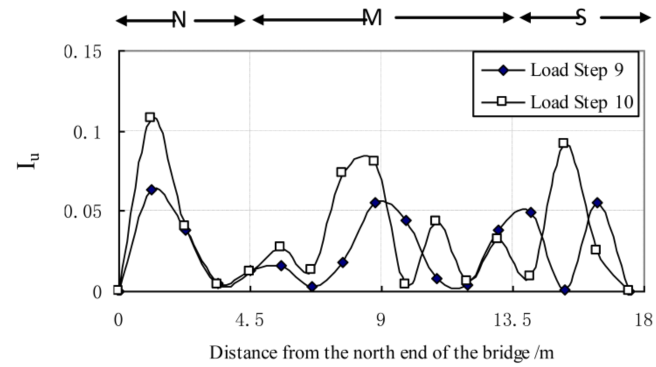


**Fig. (15).** Relative damage index change under load case D.

meters, was presented. Two load stages and ten different load steps were simulated to test various scenario of long-term loading and different levels of overload. Curvature mode method was adopted to detect damage during the exercises. It was found that the damage index of curvature mode had good capability to damage detection based on either intact structures or damaged structures. However the damage identification effect decreased when the damage was serious.

Furthermore, the finite-element model of the experimental bridge was established. By comparing the computing results and the testing results, the whole mechanical behavior including concrete cracking, steel yielding, prestreeing, contract support, and loading history could be simulated perfectly. The further analysis, such as damage prediction, could be done based on the finite-element analysis.

## CONFLICT OF INTEREST

The authors confirm that this article content has no conflict of interest.

## ACKNOWLEDGEMENTS

The authors are grateful for the Fundamental Research Funds for the Central Universities (No. FRF-TP-12-018A).

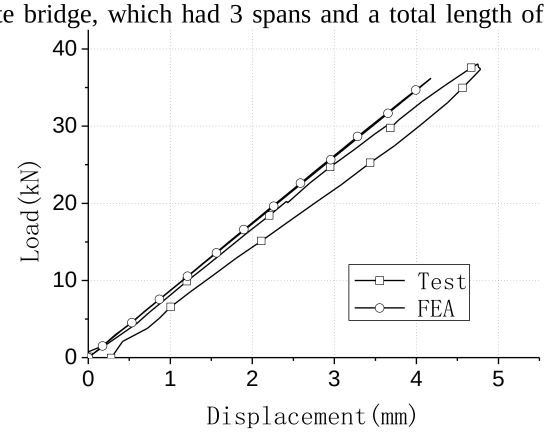


(a) Load step 1

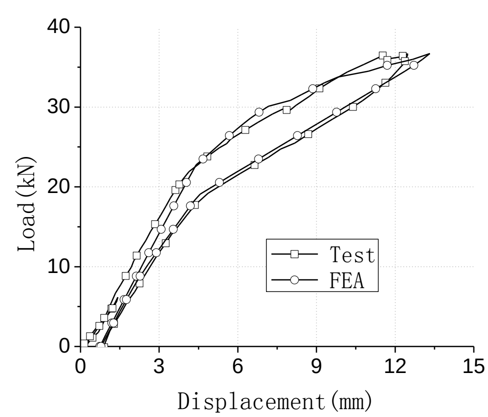


(b) Load step 2

**Fig. (16). Contd……**

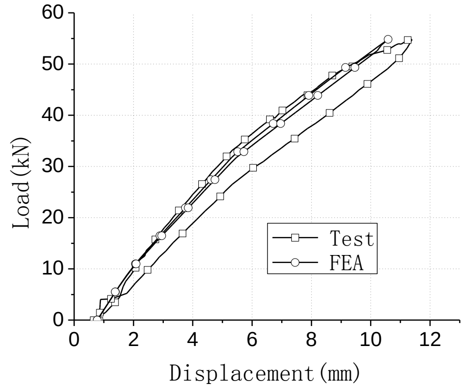


(c) Load step 3

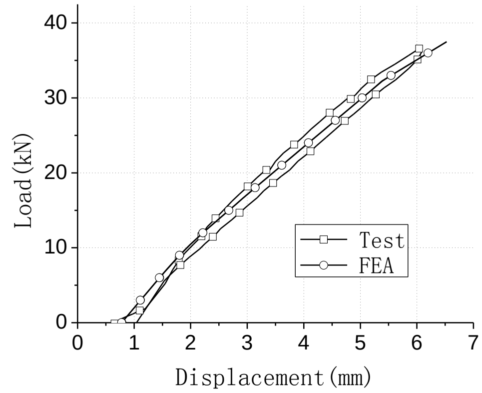


(d) Load step 4

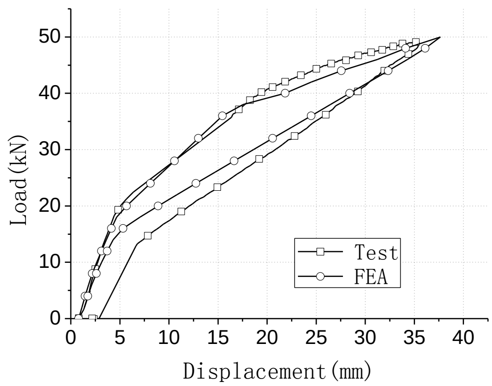


(e) Load step 5

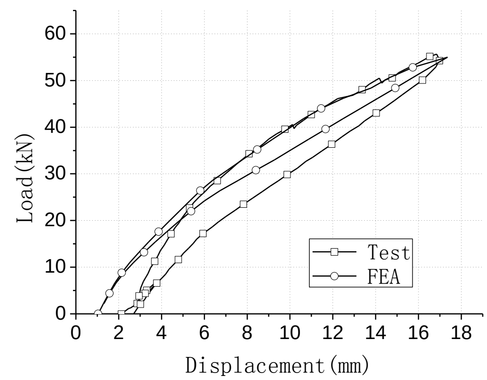


(f) Load step 6

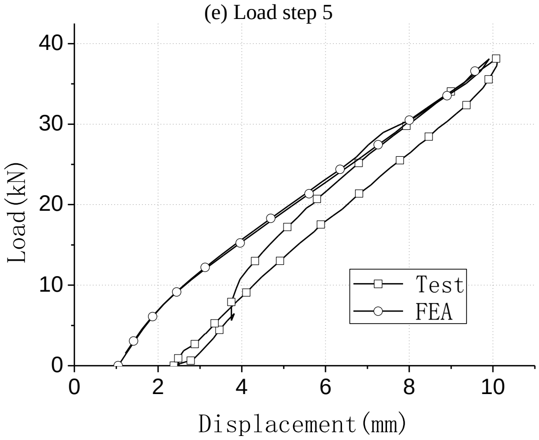


(g) Load step 7

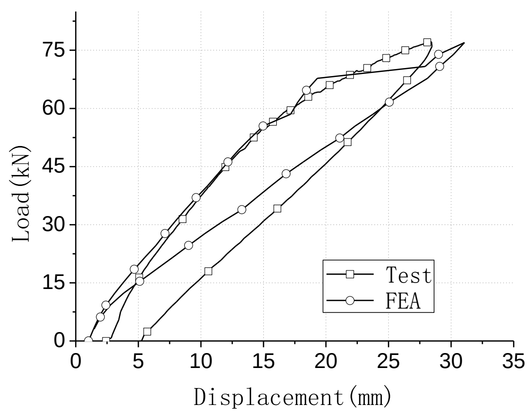


(h) Load step 8

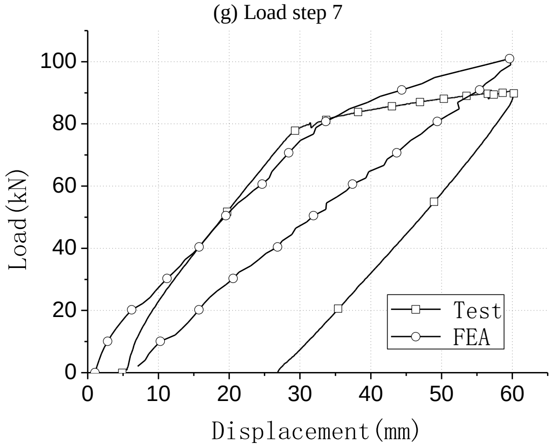


(i) Load step 9

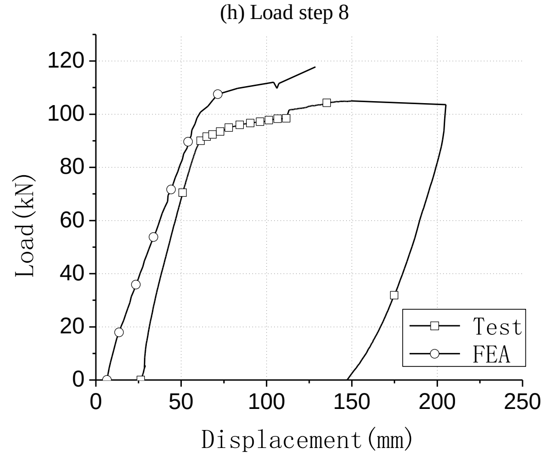


(j) Load step 10

**Fig. (16).** Load-deflection at mid-span.

## REFERENCES

[1] J. J. Jiang, X. Z. Lu, and J. J. Guo. "Study for real-time monitoring of large-span using GPS," In: Proc,3rd International Symposium on Safety Science and Technology(2002 ISSST), 2002, pp. 308-312.

[2] Q. Pei, X. Guo, and M. Z. Zhang, "A review of health monitoring and damage detection of bridge structures," *Earthquake Eng. Eng. Vib.*, vol. 23, no. 2, pp. 61-67, April 2003.

[3] H. N. Li, and D. S. Li, "Safety assessment, health monitoring and damage diagnosis for structures in civil engineering," *Earthquake Eng. Eng. Vib.*, vol. 22, no. 3, pp. 82-90, June 2002.

[4] D. B. Li, Q. H. Lu, and Y. Shi, Modal analyses and application. China Science Press: Beijing, 2001.

[5] J. K. Vandiver, "Detection of Structural failure on fixed platforms by measurement of dynamic response," In: Proceedings of the 7th annual offshore technology conference, 1975, pp. 243-252.

[6] R. D. Adams, D. X. Lin, and R. G. Ni, "Prediction and measurement of the natural frequencies and damping capacity of carbon fiber-reinforced plastics plates," *Journal de Physique (Paris), Colloque*, vol. 44, no. 12, pp. 525-530, Dec. 1983.

[7] M. Biswas, A. K. Pandey, and M. M. Samman, "Diagnostic experimental spectral/modal analysis of a highway bridge," the Int. *J. Analy. Exp. Modal Analy*, vol. 5, no. 1, pp. 33-42, Jan. 1990.

[8] O. Loland, and C. J. Dodds, "Experiences in developing and operating integrity monitoring system in North sea," In: Proceedings of the 8th Annual Offshore Technology Conference, 1976, vol. 2, pp. 313-319.

[9] M. M. Samman, M. Biswas, and A. K. Pandey. "Employing pattern recognition for detecting cracks in a bridge model," *Int. J. Analy. Exp. Modal Analy*., vol. 6, no. 1, pp. 35-44, Jan. 1991.

[10] M. Biswas, M. M. Samman, A. K. Pandey, and S. A. Bluni, "Modified chain code computer vision techniques for interrogation of vibration signatures for structural fault detection," *J. Sound and Vib.*, vol. 175, no. 1, pp. 89-104, Aug. 1994.

[11] M. M. Samman, and M. Biswa, "Vibration testing for nondestructive evaluation of bridges. I :theory," *J. Struct. Eng.*, vol. 120, no. 1, pp. 269-289, Jan. 1994.

[12] M. M. Samman, and M. Biswas. "Vibration testing for nondestructive evaluation of bridges. II :results," *J. Struct. Eng.*, vol. 120, no. 1, pp. 290-306, Jan. 1994.

[13] P. D. Cha and J. P. Tuck-Lee, "Updating structural system parameters using frequency response data," *J. Eng. Mech.*, vol. 126, no.12, 1240-1246, Dec. 2000.

[14] M. A. Mannan, and M. H. Richardson, "Detection and location of structural cracks using FRF measurements," In: Proceeding of the 8th International Modal Analysis Conference, 1990, vol. 1, pp. 652-657.

[15] Y. S. Park, H. S. Park, and S. S. Lee, "Weighted-error-matrix application to detect stiffness damage by dynamic-characteristic measurement," *Int. J. Analy. Exp. Modal Anal.*, vol. 3, no. 3, pp. 101-107, July. 1988.

[16] C. S. Lin. "Location of modeling errors using modal test data," *Am. Inst. Aeronautics J.*, vol. 28, pp. 1650-1654, Sep. 1990.

[17] H. P. Gysin, "Critical application of the error matrix method for localization of finite element modeling inaccuracies," In: Proceeding of the 4th International Modal Analysis Conference, 1986, vol. 2, pp. 1339-1351.

[18] A. K. Pandey, and M. Biswas. "Damage detection in structures using changes in flexibility," *J. Sound Vib.*, vol. 169, no. 1, pp. 3-17, Jan. 1994.

[19] A. K. Pandey, and M. Biswas. "Experimental verification of flexibility difference method for locating damage in structures," *J. Sound Vib.*, vol. 184, no. 2, pp. 311-328, July 1995.

[20] S. Rubin, and R. N. Coppolino. "Flexibility monitoring of offshore jacket platforms," In: Proceeding of the 15th Annual Offshore Technology Conference, 1983, vol. 2, pp. 201-208.

[21] D. Bernal, "Load vectors for damage localization," *J. Eng. Mech.*, vol. 128, no. 1, pp. 7-14, Jan. 2002.

[22] D. Bernal, and B. Gunes, "Damage localization in output-only systems: A flexibility based approach," In: Proceedings of IMAC-XX: Structural dynamics, 2002, pp.1185-1191.

[23] A. Nauerz, and C. P. Fritzen. "Error localization using power spectral densities," In: The 21th International Seminar on Modal Analysis (ISMA 21), Noise and Vibration Engineering, 1996, pp. 973-382.

[24] A. K. Pandey, M. Biswas, and M. M. Samman. "Damage detection from changes in curvature mode shapes," *J. Sound Vib.*, vol. 145, no. 2, pp. 312-332, March 1991.

[25] C. Sikorsky, and N. Stubbs. "Improving bridge management using NDT and quality management," In: Structural Damage Assessment Using Advanced Signal Processing Procedures, 1997, pp.399-408.

[26] M. M. A. Wahab, and G. De.Roeck. "Damage detection in bridges using modal curvatures: application to a real damage scenario," *J. Sound Vib*., vol. 226, no. 2, pp. 217-235, Sep. 1999.

[27] D. B. Li, Q. H. Lu, and Q. Qin, "Curvature modal analysis for bending structures," *J. Tsinghua Uni. (Sci. and Tech.)*, vol. 42, no. 2, pp. 224-227, Feb. 2002.

[28] A. K. Pandey, M. Biswas, and M. M. Samman, "Damage detection from changes in curvature mode shapes," *J. Sound Vib.*, vol. 145, no. 2, pp. 321-332, March 1991.

[29] X. R. Liu, J. Cai, and H. Liu, "Damage diagnosis for bridges,". China Communication Press: Beijing, 2002.

Received: March 01, 2014 Revised: March 11, 2014 Accepted: March 25, 2014